Performance Evaluation for CT-AEC:

Evaluation of the Latest CT-AEC Methods Using Dedicated Phantoms

Yoshihisa Muramatsu	*National Cancer Center East*
Nicholas Keat	*GlaxoSmithKline*
Ryo Sekine	*Tochigi National Hospital*
Shu Ikeda	*Tokai University Hospital*
Kazuaki Osawa	*Saiseikai Chuwa Hospital*
Masami Terada	*St. Luke's International Hospital*
Shigeru Miyazaki	*Toho University Omori Medical Center*
Toshi Takayama	*Kyoto Kagaku Co., Ltd.*
Noriyuki Moriyama	*National Cancer Center Research Center*

Introduction

- **While CT studies account for only 5~10% of all radiographic examinations, the effective dose associated with CT studies accounts for approximately 35~65% of the total. The use of CT automatic exposure control (CT-AEC) is very helpful in ensuring that the exposure dose is appropriate.** [1, 2, 3]
- **Since CT-AEC systems differ between manufacturers and even in the same model (Fig. 1, 2), the performance of CT-AEC systems should be evaluated using phantoms etc. before they are employed in clinical practice.**
- **Our research group has investigated the requirements for performance evaluation phantoms, has developed special phantoms, and has reported the results.**[4]
- ***The purpose of the present study was to establish a standard CT-AEC performance evaluation method by performing field tests on the latest CT-AEC systems employed by various manufacturers using special phantoms.***

1. Managing patient dose in computed tomography, ICRP Publication 87, 2000; 30
2. Mettler FA Jr et al.: CT scanning; patterns of use and dose. J Radiol Prot 2000;20:353 9
3. S J Watson et al.: HPA-RPD-001Ionising Radiation Exposure of the UK Population: 2005 Review.
4. Y Muramatsu et al.: Development of phantoms for evaluating CT-AEC, C-707/ECR06

Fig. 1: Classification of CT-AEC Systems

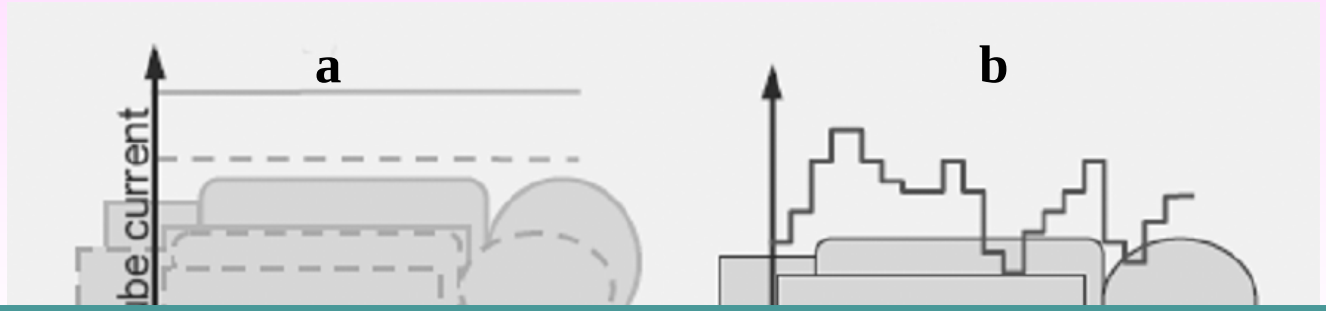

CT-AEC systems can be functionally classified into three types.

a) In patient size AEC, X-ray output (tube current) is automatically adjusted according to the patient s size.

b) In Z-axis AEC, X-ray output is adjusted for each rotation along the patient.

c) In XY AEC, X-ray output is adjusted during each rotation, according to the patient attenuation at each gantry angle.

In practice, two or more of these functions can be combined to provide

d) XYZ(3D) AEC, where the three functions described above are used in combination to modulate X-ray output.

Fig. 2: Manufacturers of CT-AEC

Manufacturer	Name	Patient size AEC	Z-axis AEC	Rotational AEC	XYZ(3D) AEC	Method for setting exposure level
GE	Smart mA	-	-	○	-	Maximum mAs is input by operator.
	Auto mA	○	○	-	-	"Noise Index" sets required image noise level for 'standard' kernel.
	3D mA	○	○	○	○	
Hitachi	Adaptive-mA	-	○	○	-	Maximum mAs is input by operator without Scanogram.
Philips	ACS	○	-	-	-	
	Z-DOM	○	○	-	-	"Reference mAs" is set for standard-sized patient.
	D-DOM	○		○		

Various types CT-AEC systems are employed by different manufacturers.

Their principles of operation differ depending on the release date and the version.

In addition, there are two image-quality setting methods for reconstructed images: in one method, the user enters a numerical value derived from the image noise, and in the other method, a standard mAs value is set for a reference target.

Methods 1

1. Areas for performance evaluation

Patient size characteristics in the Z-axis direction

Patient shape characteristics in the XY plane

Impulse response characteristics

2. Basic description of four type phantoms for CT-AEC

(Kyoto Kagaku, Kyoto, Japan)

All of these phantoms are made of acrylic.

Cone phantom (Fig. 3): Evaluates performance for different patient sizes, and where the patient size changes along the z-axis

Elliptical cone phantom (Fig. 4): As above, but also shows the benefit of XY AEC

Variable-XY phantom (Fig. 5): Evaluates performance of XY AEC as cross section changes from circular to highly elliptical

Stepped phantom (Fig. 6): Evaluates the performance of the AEC to sudden changes in patient cross section

Fig. 3: Cone Phantom

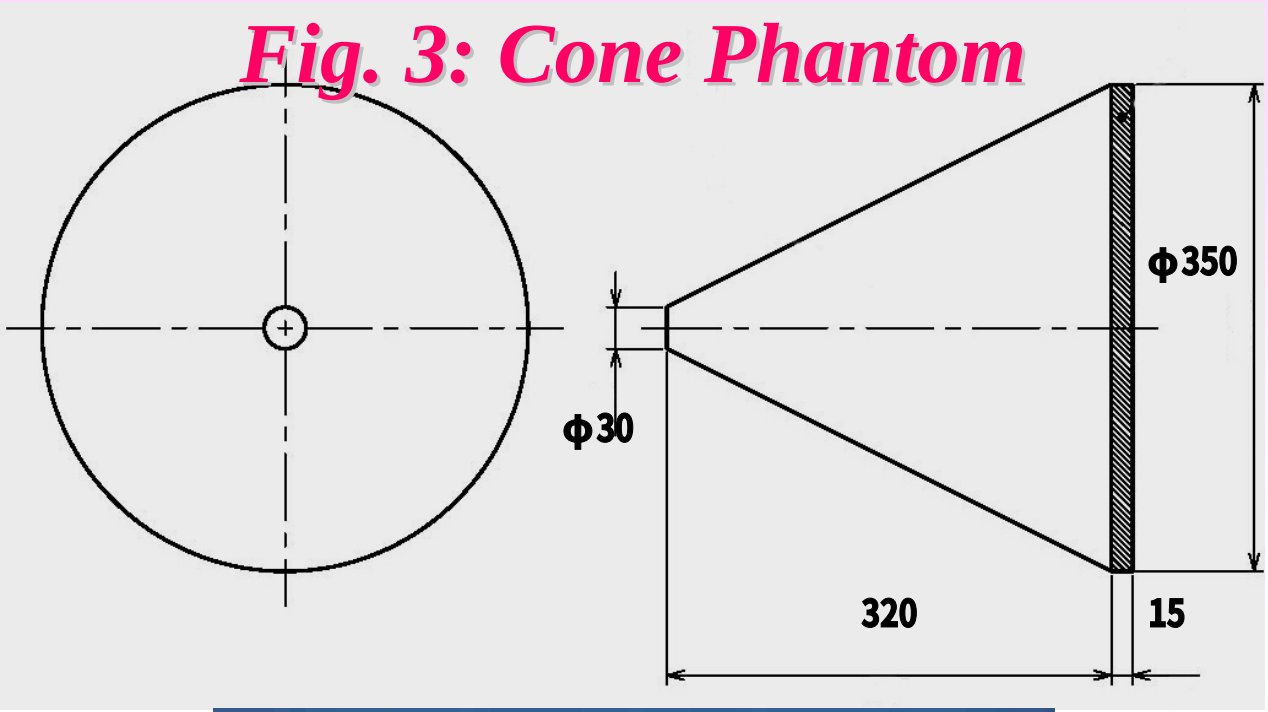

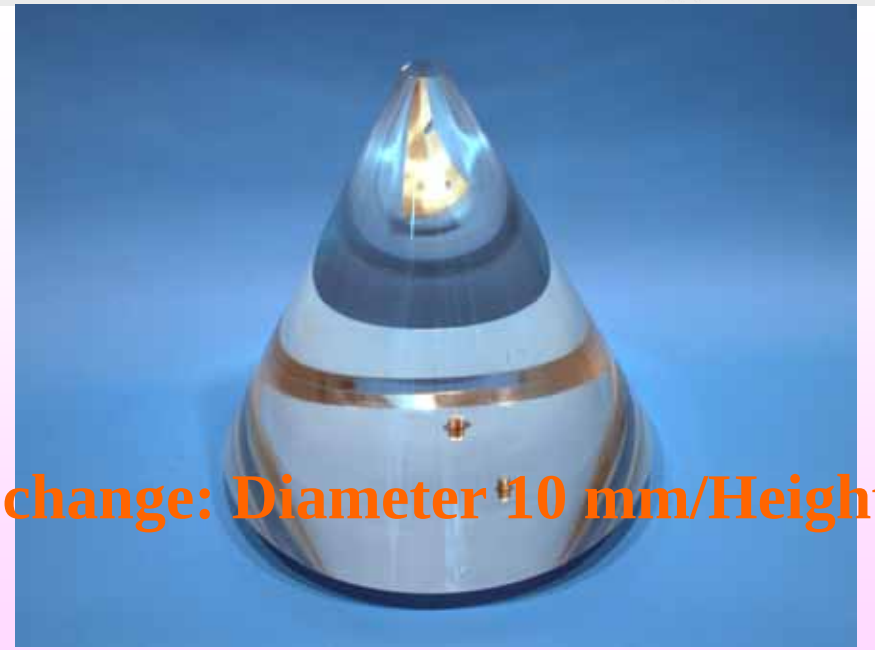

*** Note**

Rate of change: Diameter 10 mm/Height 10 mm

Fig. 4: Elliptical Cone Phantom

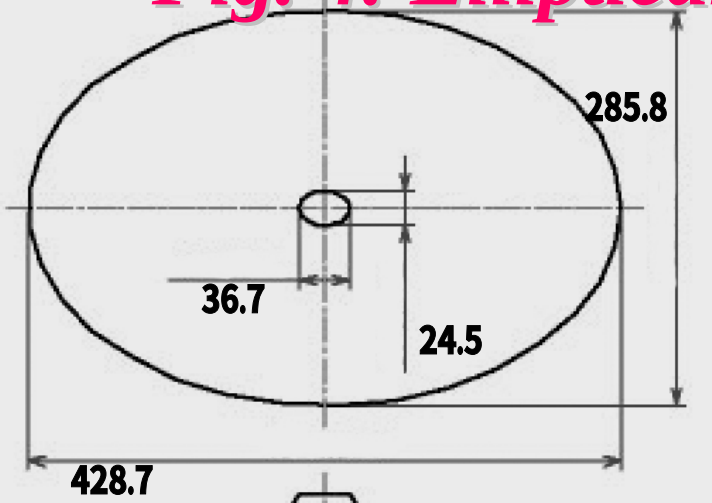

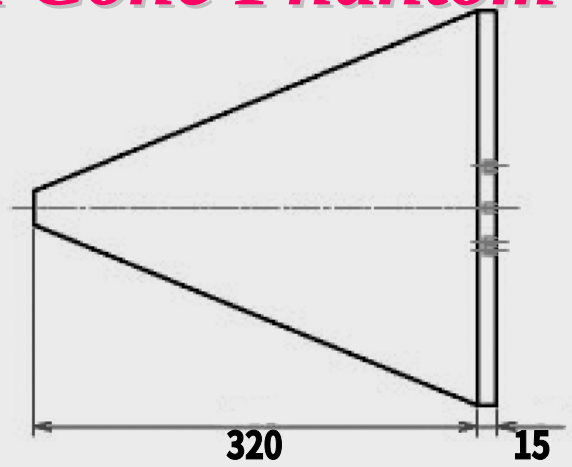

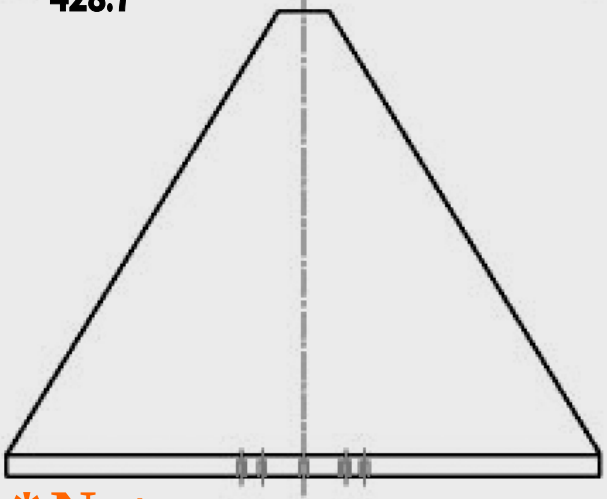

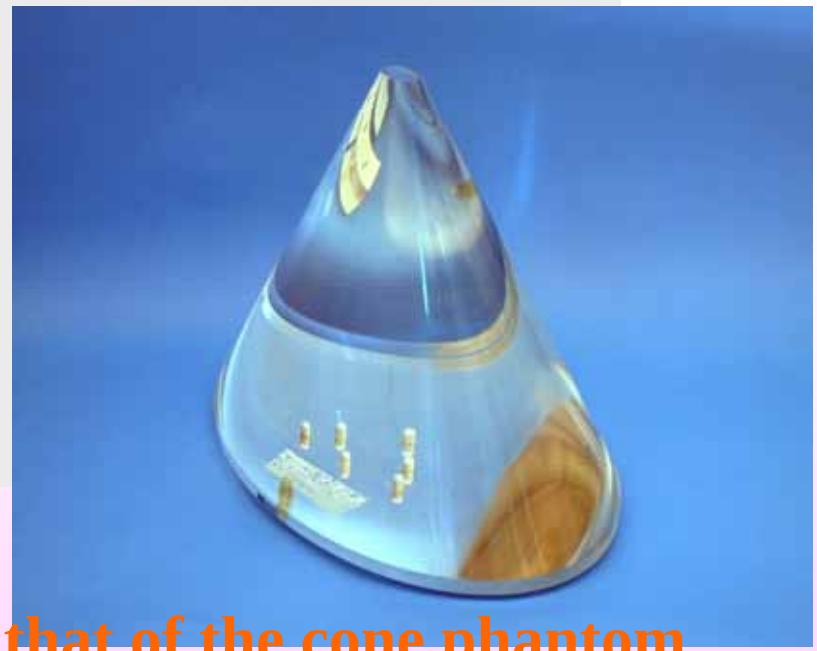

*** Note**

X-Y ratio of 1:1.5

Sectional area equal to that of the cone phantom

Fig. 5: Variable-XY Phantom

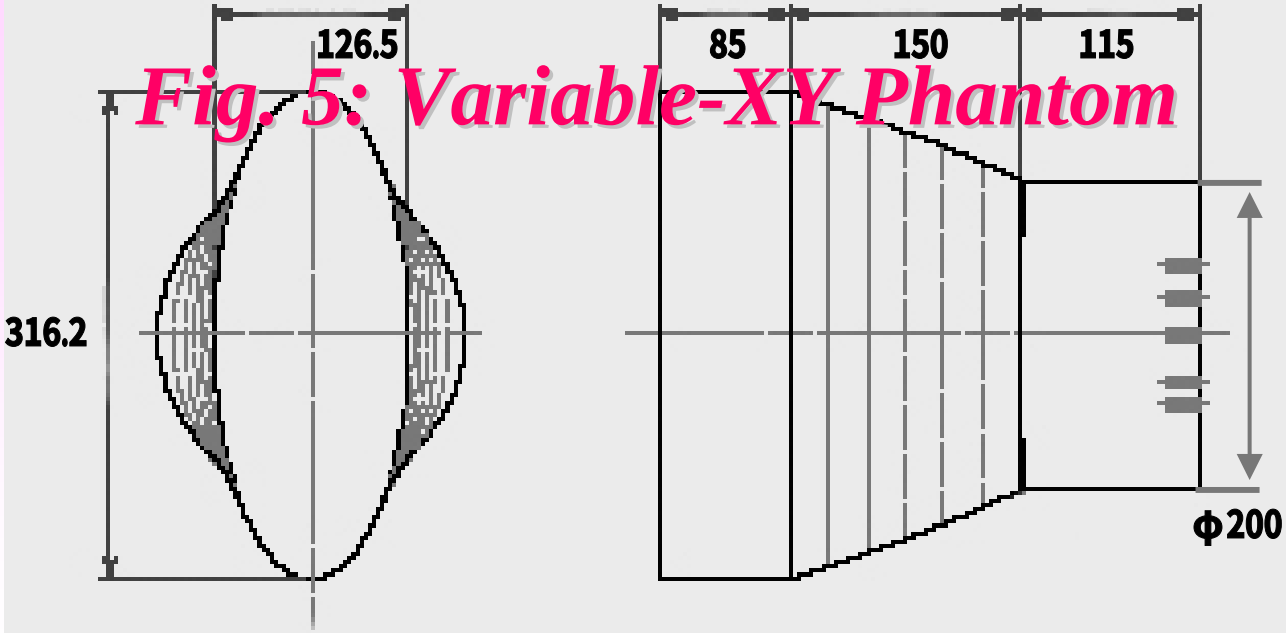

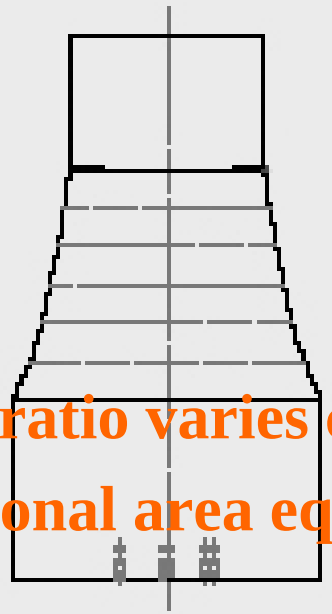

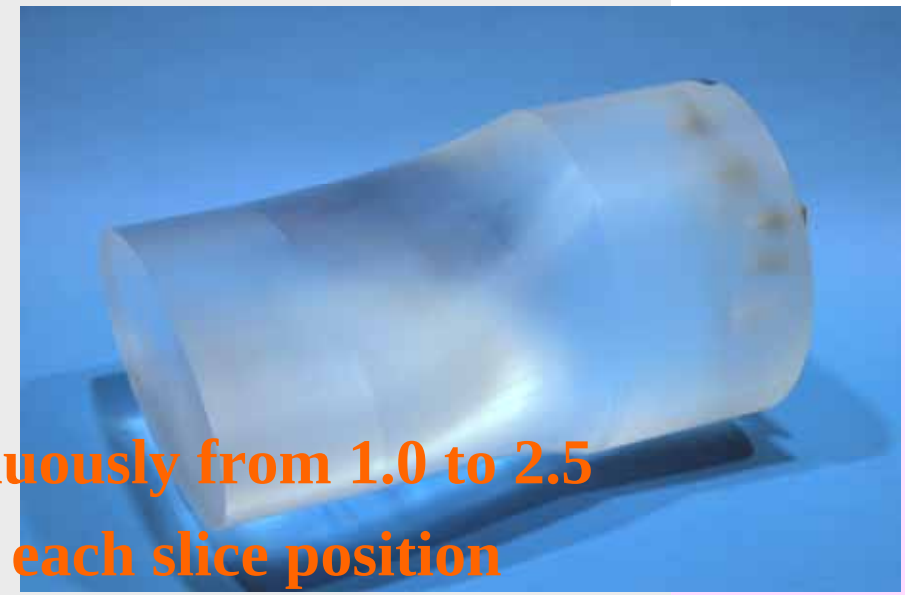

*** Note**

X-Y ratio varies continuously from 1.0 to 2.5

Sectional area equal at each slice position

Fig. 6: Stepped Phantom

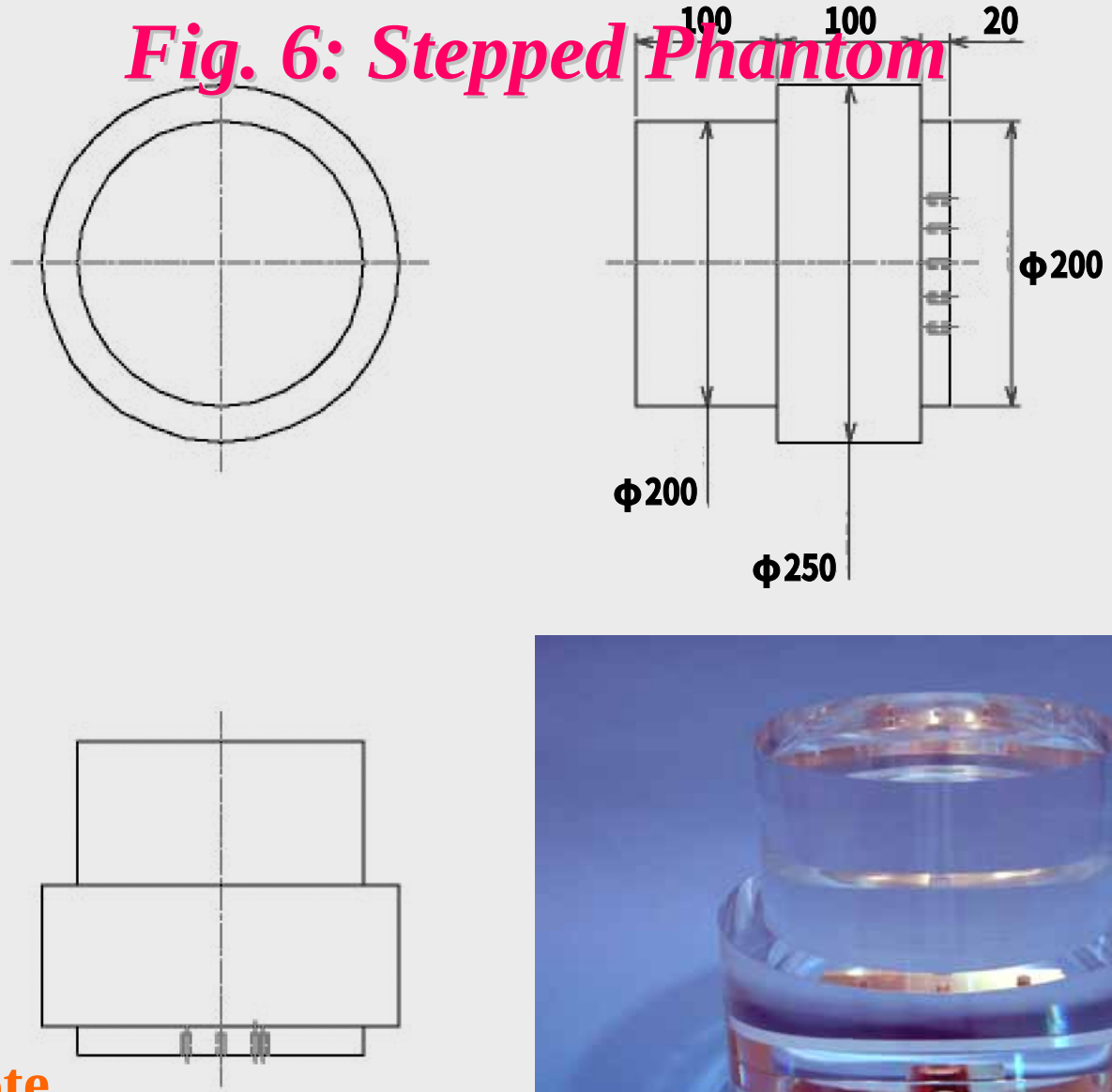

* Note

Diameter difference of 50 mm

Methods 2

3. Targets for field tests

The field test targets were seven types of CT-AEC systems installed in four CT scanners as listed below by alphabetical order of manufacture.

For the Dose Right system, ACS was used in combination taking into account the system status when used in clinical practice.

LightSpeed VCT, GE, USA: ***Auto mA*, Auto mA + Smart mA*****

****: shown as "2D mA", **: shown as "3D mA"***

Brilliance 16P, Phillips, Netherlands: ***Dose Right ACS+D-DOM, Z-DOM***

Sensation 64, Siemens, Germany: ***CARE Dose 4D***

Aquilion 64M, Toshiba, Japan: ***Sure Exposure, Volume-EC***

Methods 3

4. Data acquisition

Each phantom was positioned using a phantom holder so that its cross section was parallel to the scan plane and its central axis was aligned with the gantry rotation center (Fig. 7).

The scan conditions were determined for each CT scanner assuming that CT studies for the chest and abdomen were to be performed.

Details concerning the scan conditions for various CT-AEC systems are shown in Fig. 8.

Note that scans were acquired without CT-AEC for comparison.

Images were reconstructed from the acquired raw data sets, and special software (GETROI, BioArts, Japan) was used to read the tube current values in the DICOM Tag and to calculate the image noise (ROI-SD, Fig. 9).

Fig. 7: Phantom Setting

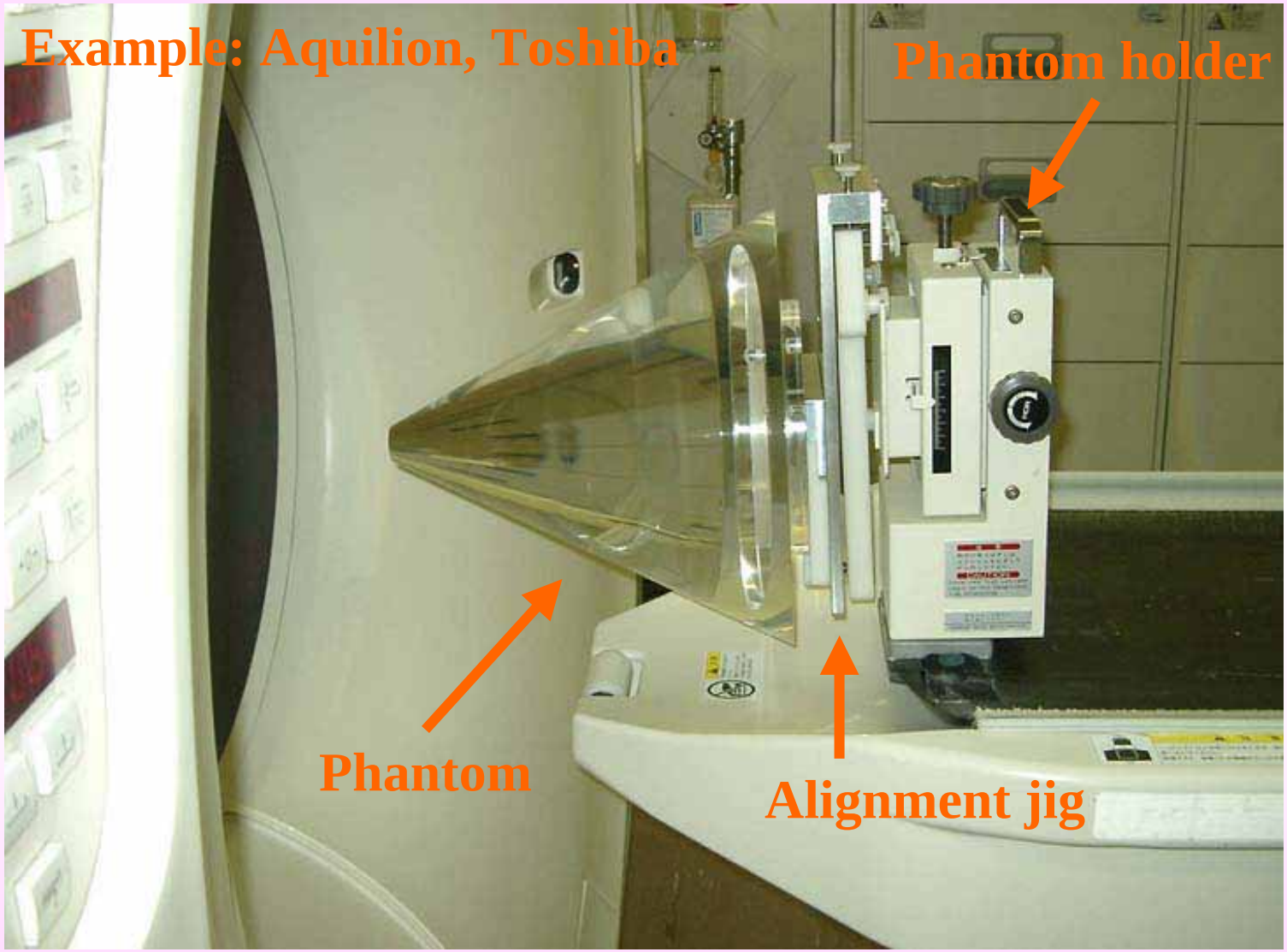

Fig. 8: Basic Conditions for Typical Body Helical Scanning

CT-AEC: CT Scanners (alphabetical order of manufactures)

Parameters	Auto mA, 3D mA : LightSpeed VCT	Dose Right : Brilliance16P	Care Dose 4D : Sensation 64	Sure Exposure : Aquilion 64M
kV	120	120	120	120
Ref. mAs	–	##	280	–
SD setting	NI: 6, 7, 12#	–	–	SD: 10.0
s/rot.	0.5	0.75	0.5	0.5
Kernel	Standard	B	B31f	FC13
row*DAS	0.625mm*32/64	0.75mm*16	0.6mm*64	0.5mm*64
Beam Width	20/40	12mm	19.2mm	32mm
Pitch factor	1.375	0.6875	0.5	0.625
Other			Moderation factor	

Common Parameters (Values in parentheses are for the stepped phantom.)

DFOV:	400 mm	Image slice:	5 mm
Recon. interval:	5 mm (1 mm)	Scanning range:	200 mm (100 mm)
Direction:	IN (IN, OUT)		

#: Adjusted accordingly
##: Adjusted by ACS

Fig. 9: Automatic ROI-SD Calculations

Example: Variable-XY Phantom

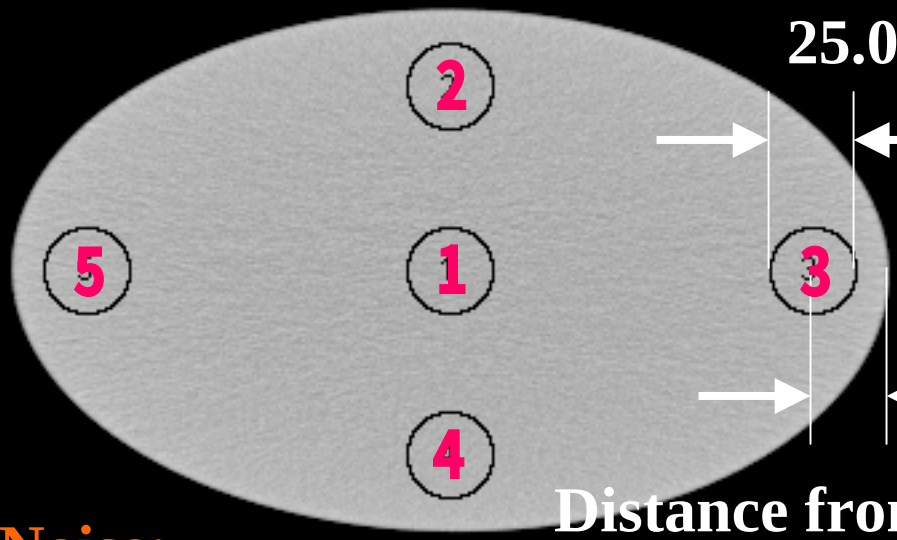

Image Noise:

"ROI-SD" = $\Sigma SD_{1\sim5}/5$

(Stepped phantom uses with Center SD_1)

Result 1-1: GE
Auto mA, 3D mA (LightSpeed VCT)

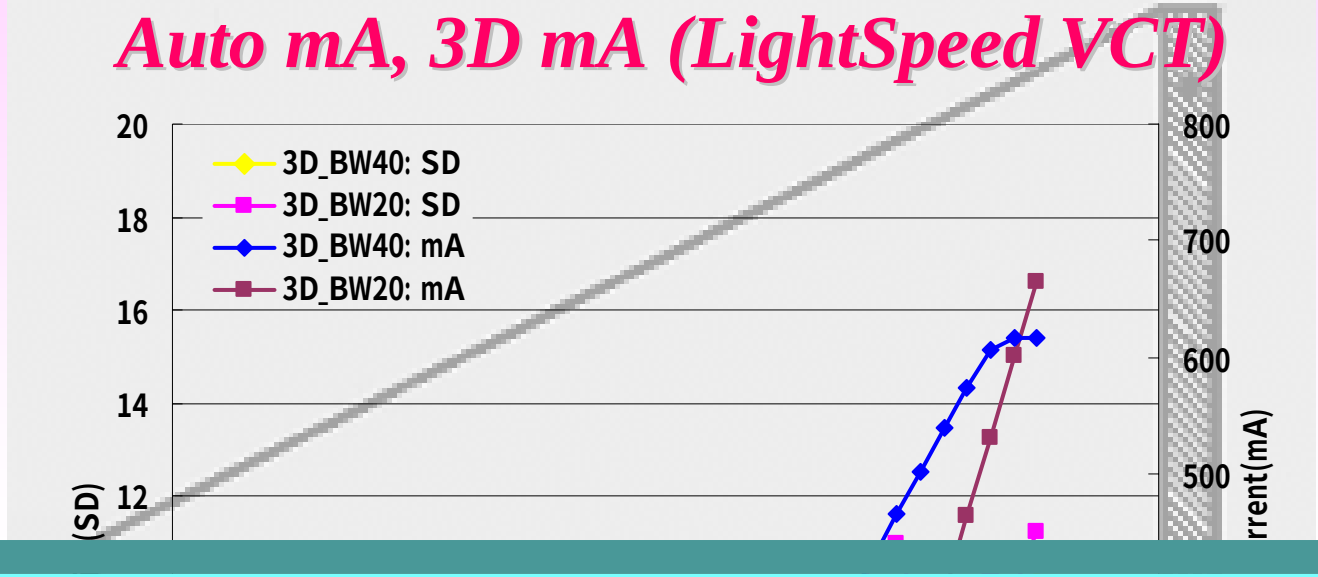

Figure 10 shows the patient size characteristics of 3D mA when the cone phantom was scanned in the IN direction (from the small-diameter end to the large-diameter end). The noise index (NI) was 12.0.

The ROI-SD showed an almost constant value of approximately 9.0 for a beam width (BW) of 20 mm or approximately 6.2 for a BW of 40 mm as the diameter varied in the range from 100 mm to 250 mm. For a BW of 40 mm, a tube current value approximately twice that for a BW of 20 mm was selected.

Result 1-2: GE
Auto mA, 3D mA (LightSpeed VCT)

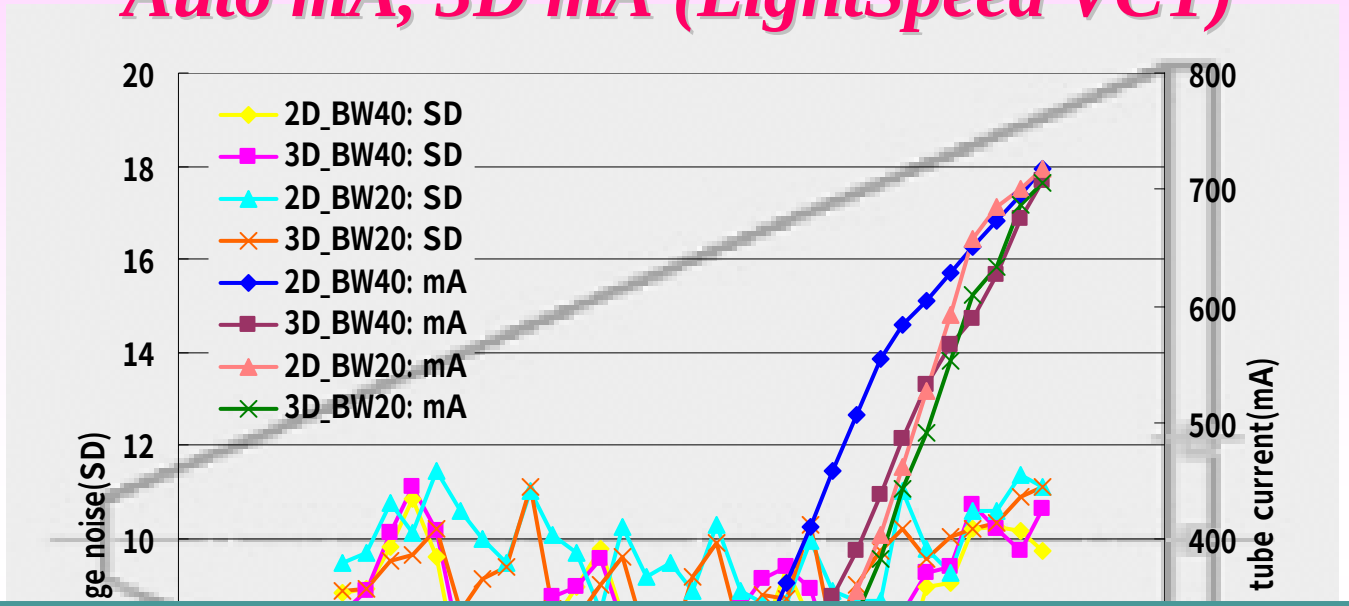

Figure 11 shows the patient size characteristics obtained when the elliptical cone phantom was scanned in the IN direction.

The NI was 12.0, as in the case for the cone phantom, and the ROI-SD was lower than the NI value.

The variation was more significant for a BW of 40 mm than for a BW of 20 mm.

In addition, there was almost no difference between 2D and 3D mA.

Result 1-3: GE
Auto mA, 3D mA (LightSpeed VCT)

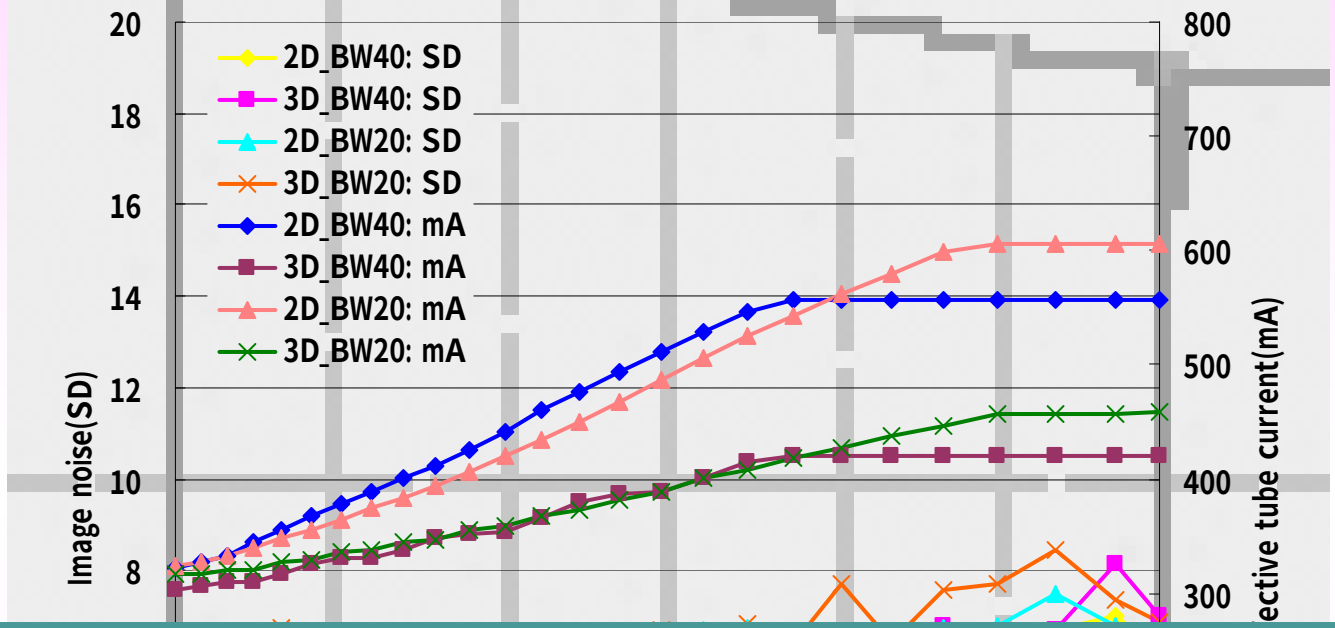

Figure 12 shows the patient shape characteristics obtained when the variable-XY phantom was scanned in the IN direction.

The NI was 6.0.

The ROI-SD showed slight variation when the vertical-to-horizontal ratio was 2.0 or more, but was stable regardless of the BW for both 2D and 3D mA.

Result 1-4: GE
Auto mA, 3D mA (LightSpeed VCT)

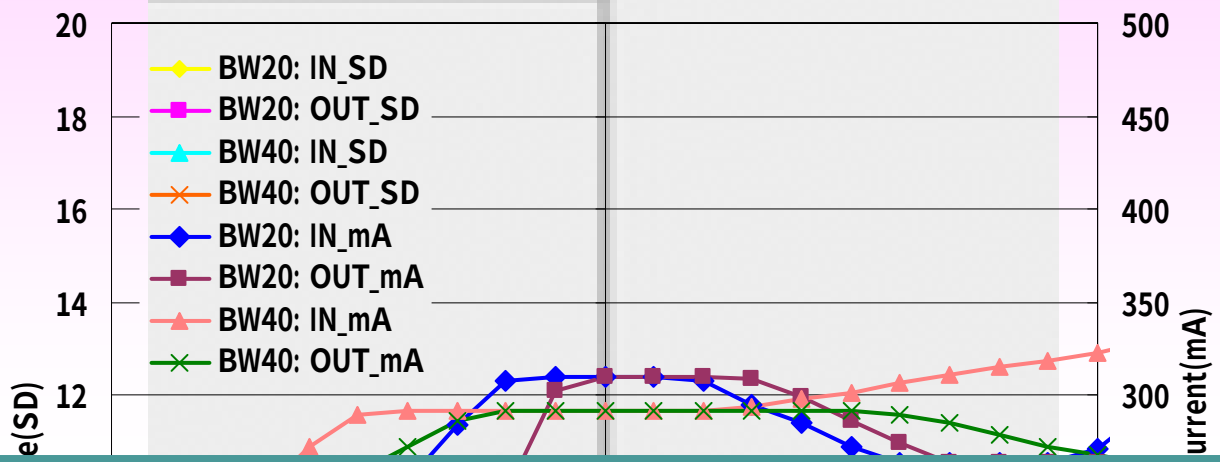

Figure 13 shows the response characteristics of 3D mA when the stepped phantom was scanned. The NI was 7.0. The pitch factors were BW 20 mm: 0.969 and 40 mm: 0.984. In IN (from the small-diameter end to the large-diameter end) scanning, the ROI-SD showed a value lower than NI before the origin point where the phantom diameter changed, while in OUT (from the small-diameter end to the large-diameter end) scanning, the ROI-SD showed a value lower than NI after the origin point. This tendency was more pronounced for BW 40 mm.

Result 2-1: Phillips Dose Right (Brilliance 16P)

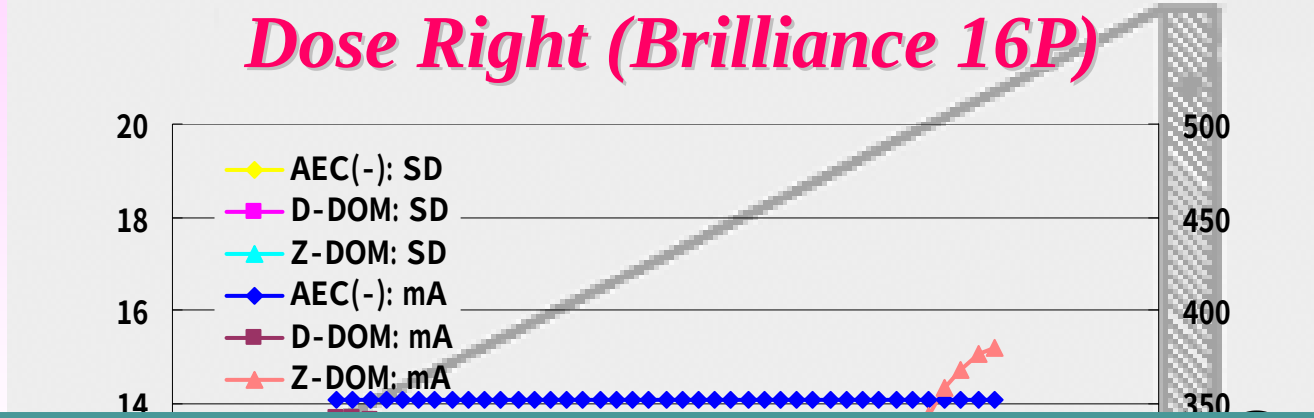

Figure 14 shows the patient size characteristics obtained when the cone phantom was scanned in the IN direction.

For D-DOM, the maximum phantom diameter in the scan range was handled as the maximum tube current (340 mA), and the tube current did not vary as the diameter changed. The ROI-SD showed the same value as with AEC Off. On the other hand, the tube current changed in the range between the maximum and approximately 70% of the maximum (125 mA) when the phantom diameter varied, showing a gradual increase in the ROI-SD as the phantom diameter increased from 200 mm to 300 mm.

Result 2-2: Phillips Dose Right (Brilliance 16P)

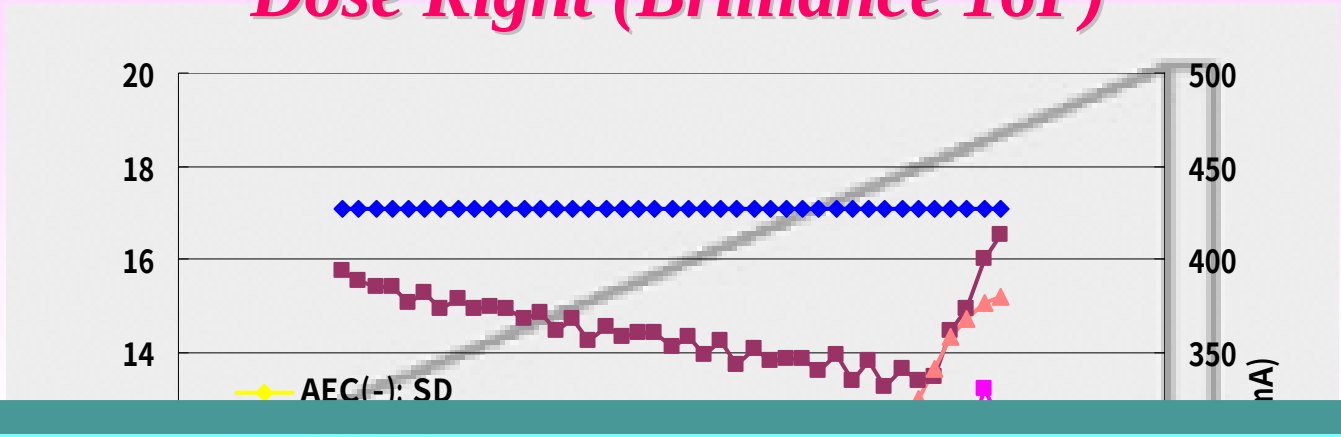

Figure 15 shows the patient size characteristics obtained when the elliptical cone phantom was scanned in the IN direction.

The ROI-SD for D-DOM was almost equal to that with AEC Off despite a tube current lower than that with AEC Off. For Z-DOM (+Adaptive Filter), the tube current as the phantom diameter varied was equal to that for the cone phantom (Fig. 14). However, the ROI-SD showed an almost constant low value in the range from 200 mm to 300 mm in phantom diameter, i.e., from the maximum tube current to approximately 70% of the maximum tube current (125 mA).

Result 2-3: Phillips Dose Right (Brilliance 16P)

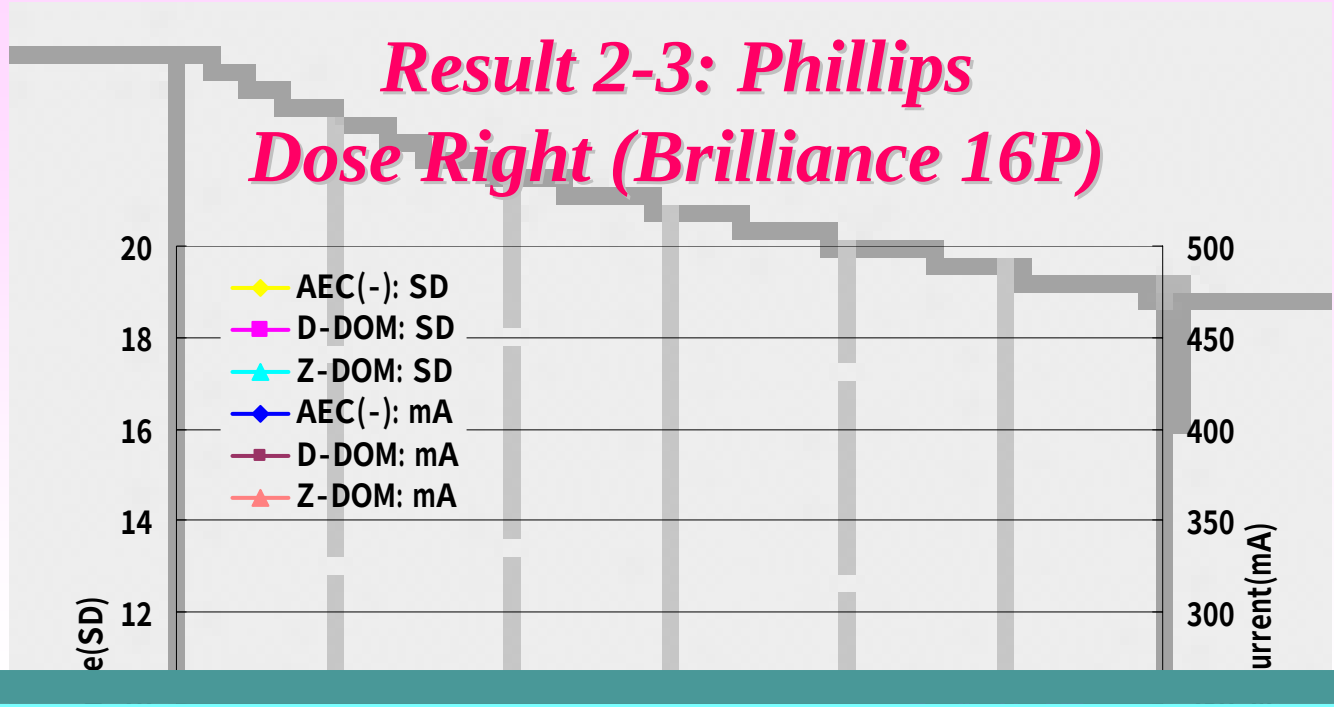

Figure 16 shows the patient shape characteristics obtained when the variable-XY phantom was scanned in the IN direction.

As in Fig. 15, the ROI-SD for D-DOM was almost equal to that with AEC Off despite a tube current lower than that with AEC Off.

On the other hand, the tube current for Z-ROM (-Adaptive Filter) showed an almost constant value as the phantom diameter varied.

The ROI-SD was almost equal to that with AEC Off.

Result 2-4: Phillips Dose Right (Brilliance 16P)

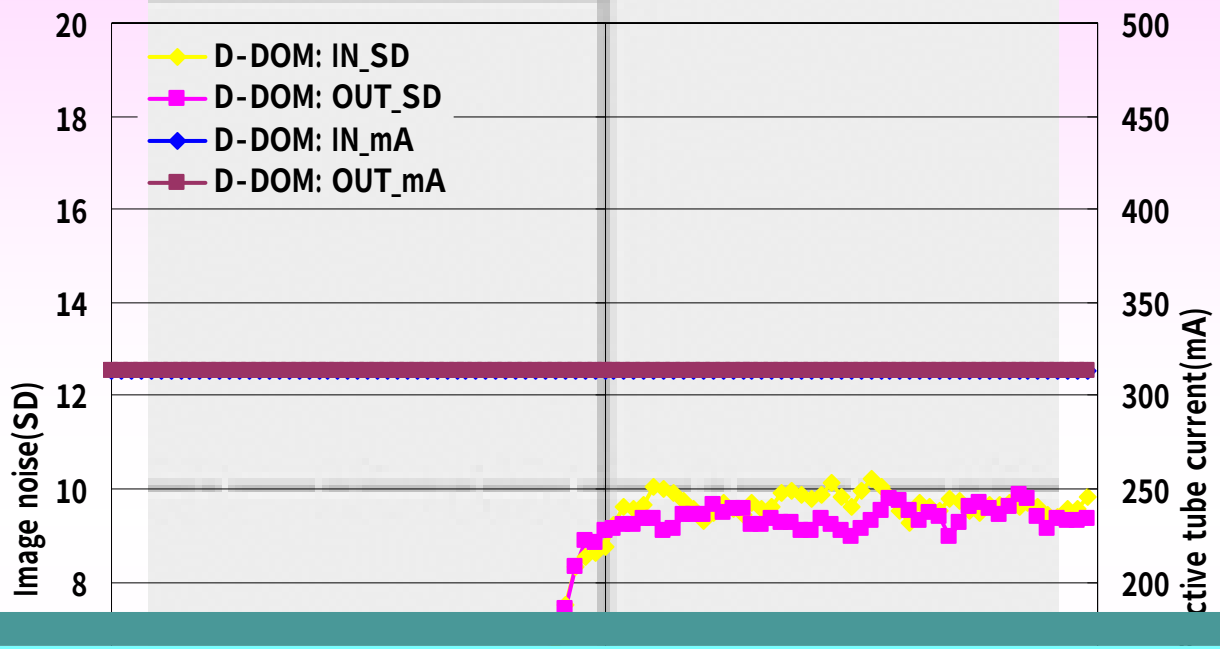

Figure 17 shows the response characteristics of D-DOM when the stepped phantom was scanned.

In both IN and OUT scanning, the ROI-SD changed significantly at the origin point (where the phantom diameter changed), with values of approximately 5.5 and 9.5 at the small-diameter end and the large-diameter end, respectively.

Result 3-1: Siemens Care Dose 4D (Sensation 64)

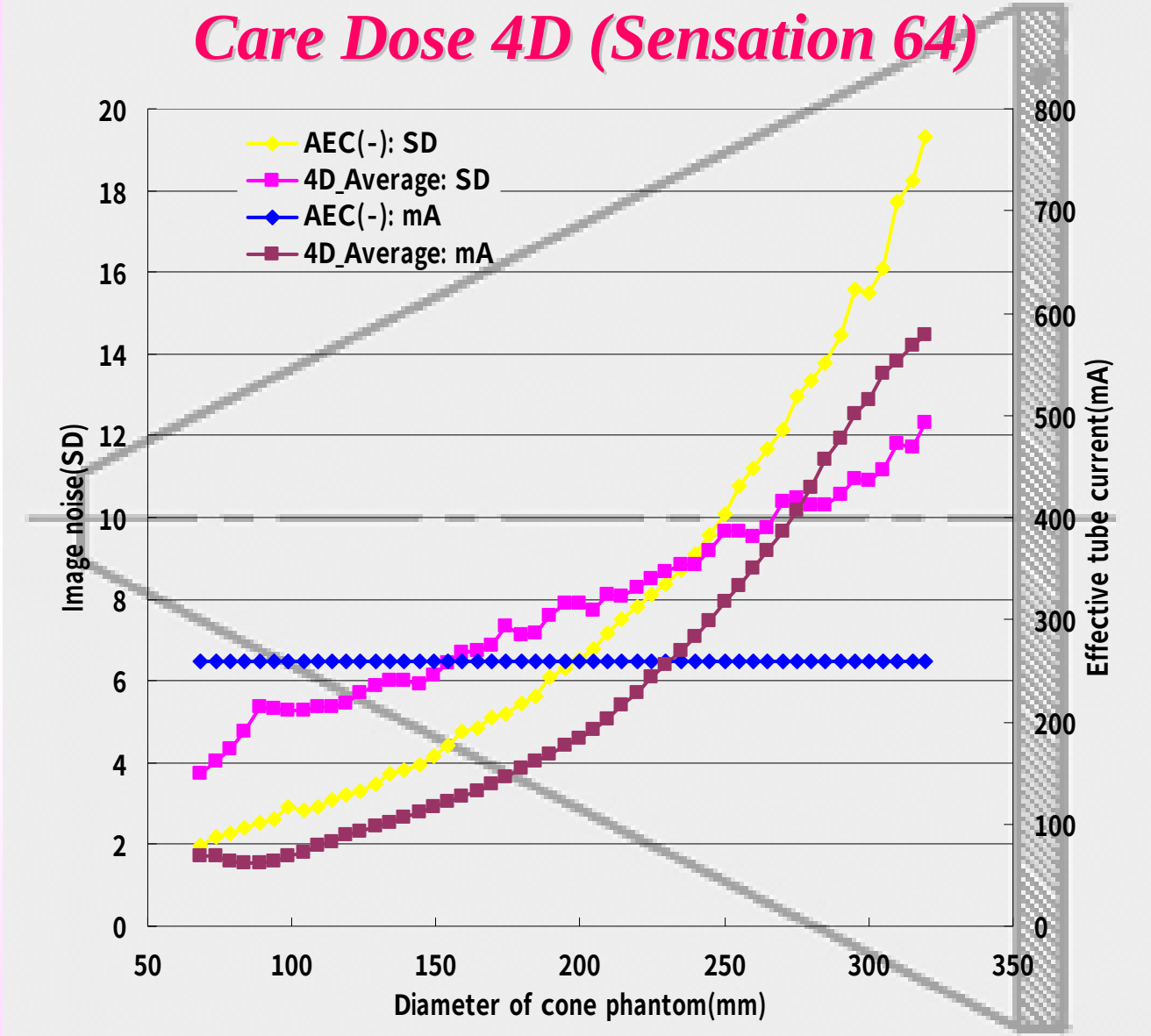

Cone phantom at IN direction: Fig. 18

Result 3-2: Siemens Care Dose 4D (Sensation 64)

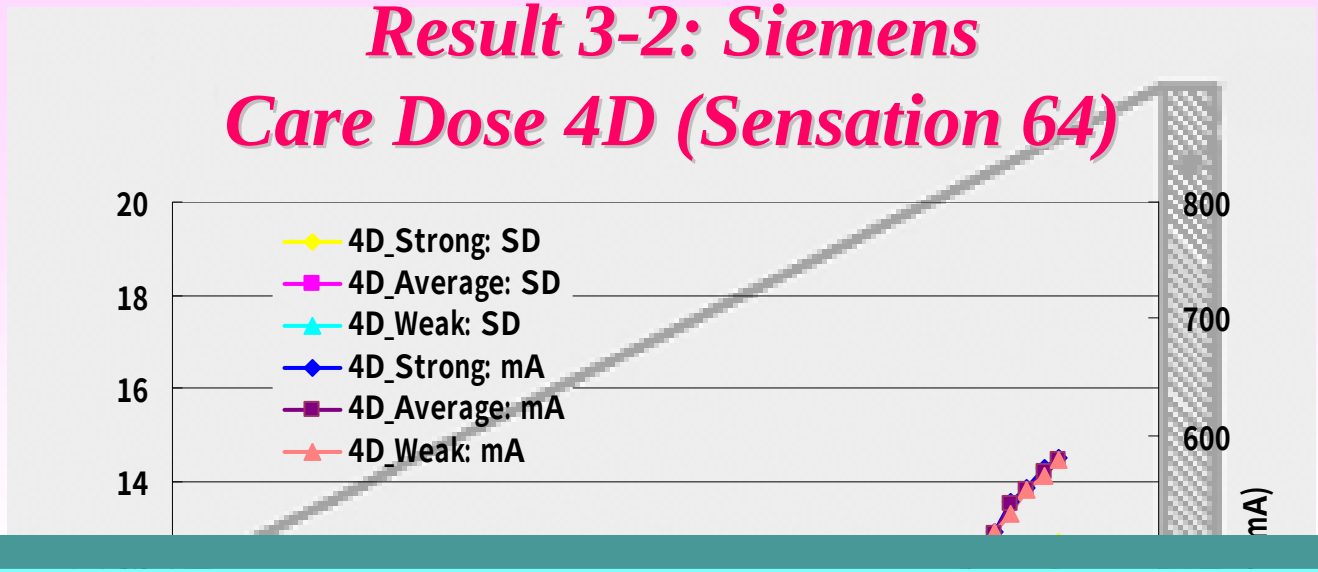

Figure 18 shows the results of comparison between Average and AEC Off (effective mAs 170) with regard to the patient size characteristics obtained when the cone phantom was scanned in the IN direction. Similarly, Fig. 19 shows the results of comparisons between the three types of modulation intensity factors (Strong, Average, and Weak) under the same conditions.

With CARE Dose 4D, the ROI-SD increased more gradually than with AEC Off as the phantom size (diameter) increased. In addition, the degree of increase differed depending on the modulation intensity factor.

Result 3-3: Siemens Care Dose 4D (Sensation 64)

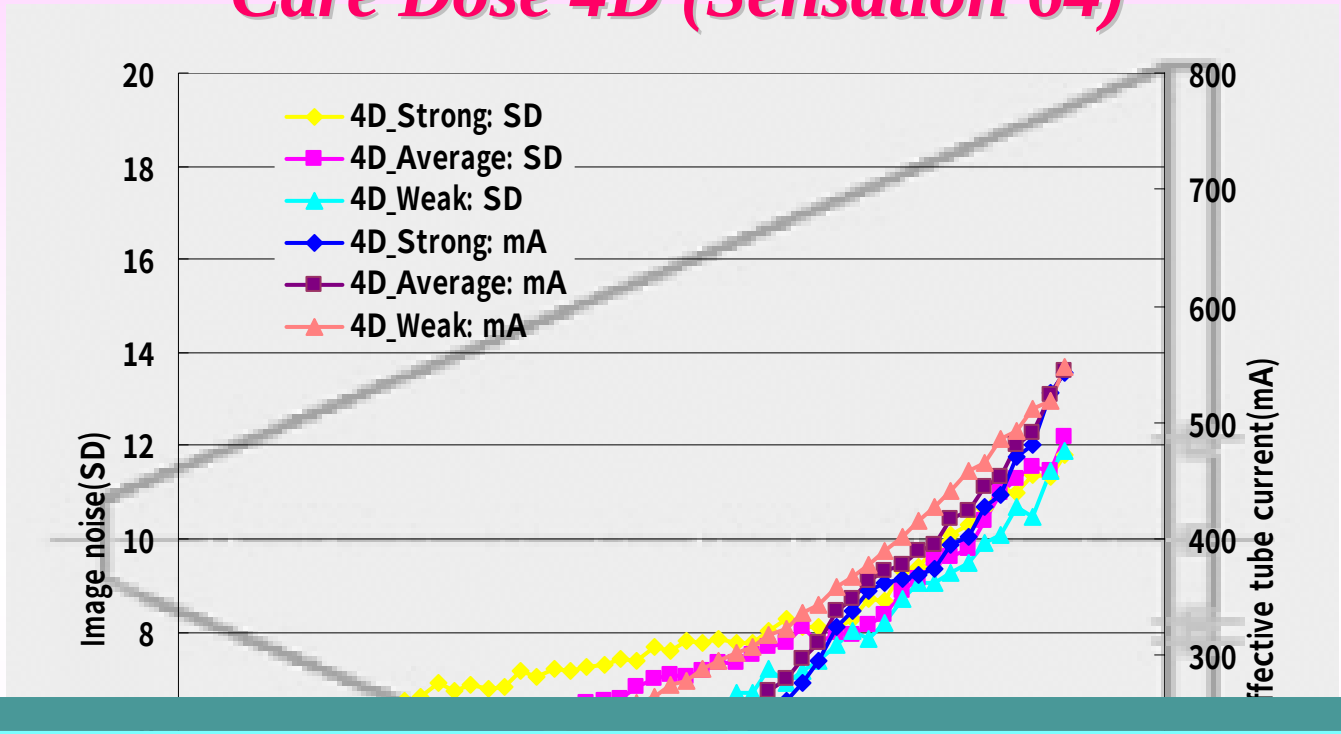

Figure 20 shows the the results of comparisons between the modulation intensity factors with regard to the patient size characteristics obtained when the elliptical cone phantom was scanned in the IN direction.

The ROI-SD showed the same trends for both the elliptical cone phantom and the cone phantom, but it was generally smaller for the elliptical phantom.

Result 3-4: Siemens Care Dose 4D (Sensation 64)

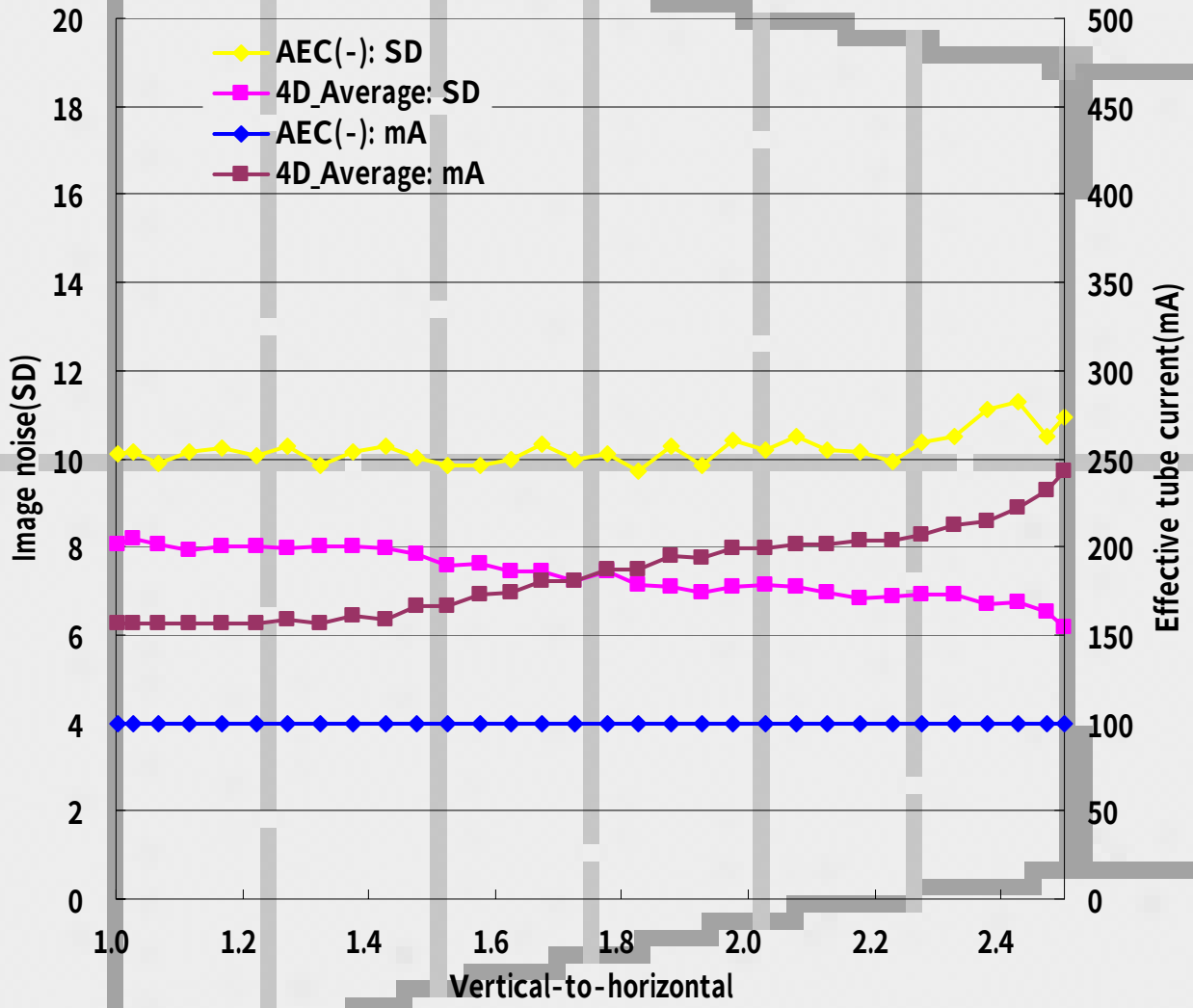

Variable-XY phantom at IN direction: Fig. 21

Result 3-5: Siemens Care Dose 4D (Sensation 64)

Figure 21 shows the the results of comparisons between Average and AEC Off (effective mAs 50) with regard to the patient shape characteristics obtained when the variable-XY phantom was scanned in the IN direction. Figure 22 shows the the results of comparisons between the modulation intensity factors under the same conditions.

With AEC Off, the ROI-SD was 10.0 when the vertical-to-horizontal ratio was 1.0, while it was 12.0 when the vertical-to-horizontal ratio was 2.5, indicating that the ROI-SD increased gradually as the vertical-to-horizontal ratio increased.

For CARE Dose 4D, however, the ROI-SD decreased as the vertical-to-horizontal ratio increased.

In addition, the ROI-SD was more strongly modulated in the order "Strong", "Average", and "Weak". The modulation level for Weak was the lowest, and its ROI-SD showed an almost constant value.

Result 3-6: Siemens Care Dose 4D (Sensation 64)

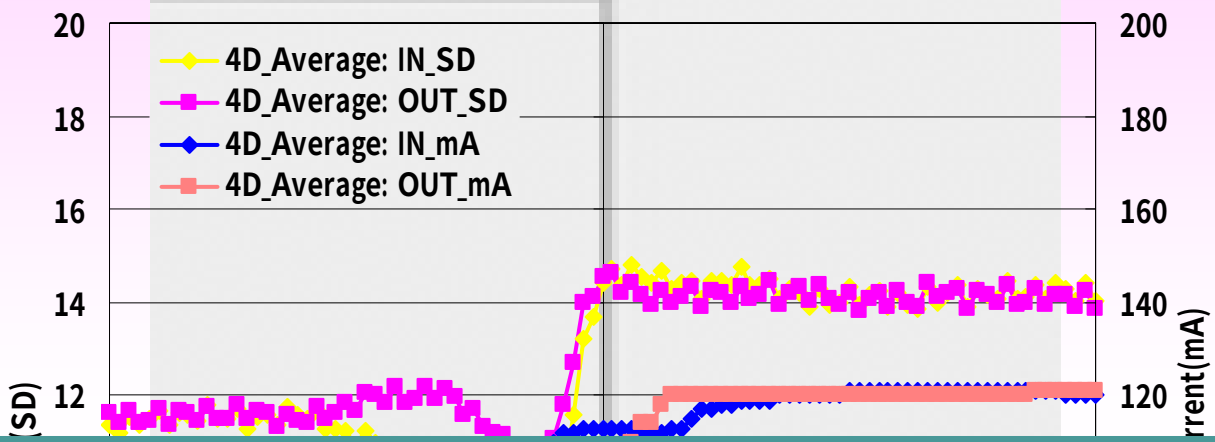

Figure 23 shows the response characteristics of CARE Dose 4D when the stepped phantom was scanned. The standard scan conditions were changed to 1.0 s/rot., pitch factor 1.0, and Ref. mAs 235.

In both the IN and OUT directions, the ROI-SD showed a lower value in the range of 10 mm to 20 mm from the origin point at the small-diameter end. For other ranges, however, the ROI-SD showed a constant value of approximately 12 at the small-diameter end and 14 at the large-diameter end.

Result 4-1: Toshiba Sure Exposure, Volume-EC (Aquilion 64M)

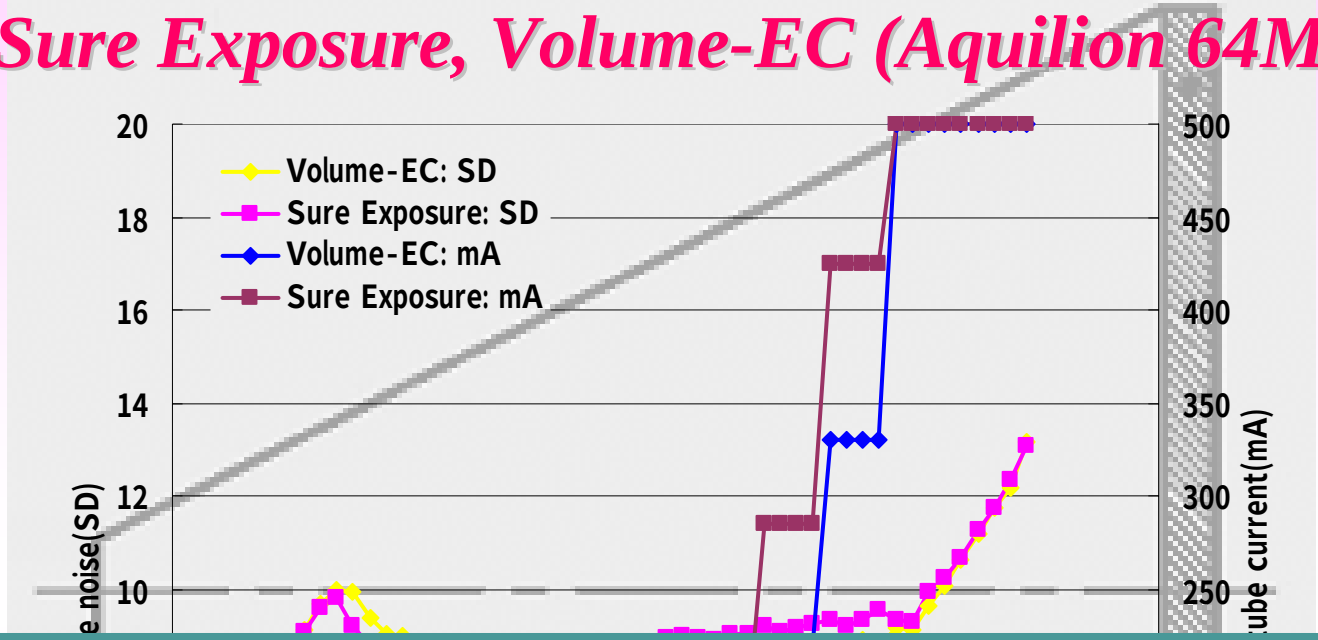

Figure 24 shows the patient size characteristics obtained when the cone phantom was scanned in the IN direction.

For both Sure Exposure and Volume-EC, the ROI-SD showed an almost constant value of 9.0 as the size (diameter) varied in the range from 90 mm to 280 mm, but increased when the diameter exceeded 280 mm, at which the maximum tube current of 500 mm was set.

Result 4-2: Toshiba
Sure Exposure, Volume-EC (Aquilion 64M)

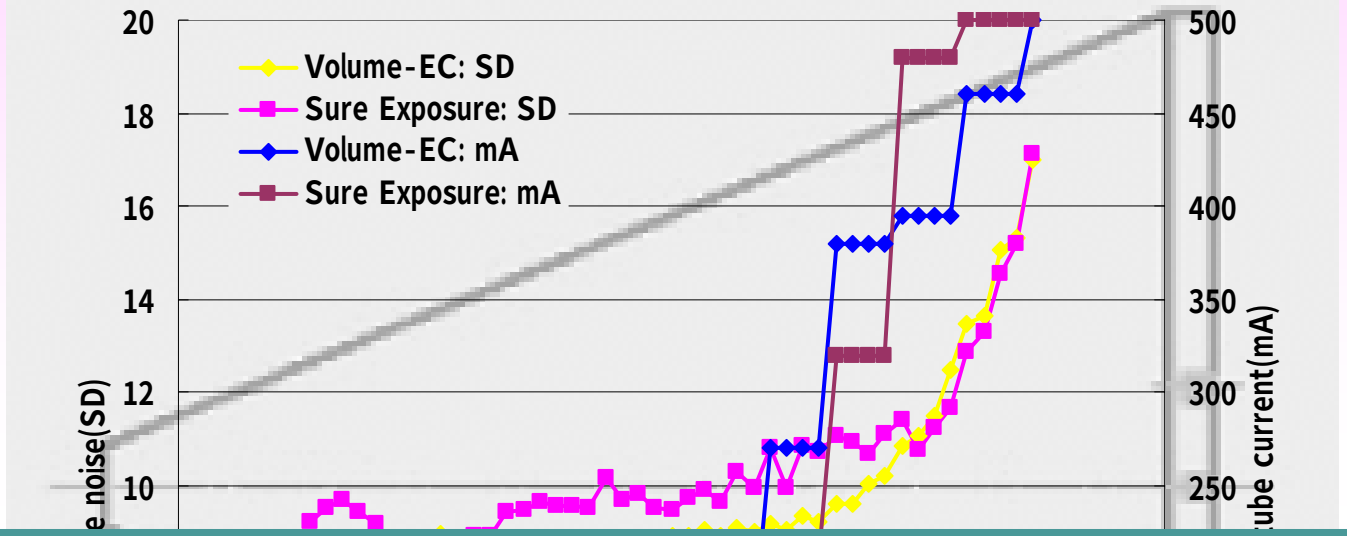

Figure 25 shows the patient size characteristics obtained when the elliptical cone phantom was scanned in the IN direction.

For Sure Exposure, the ROI SD gradually increased as the diameter became larger.

For Volume-EC, the ROI-SD showed an almost constant value of approximately 8.9 as the diameter varied in the range from 100 mm to 260 mm, but increased when the diameter exceeded 260 mm.

Result 4-3: Toshiba Sure Exposure, Volume-EC (Aquilion 64M)

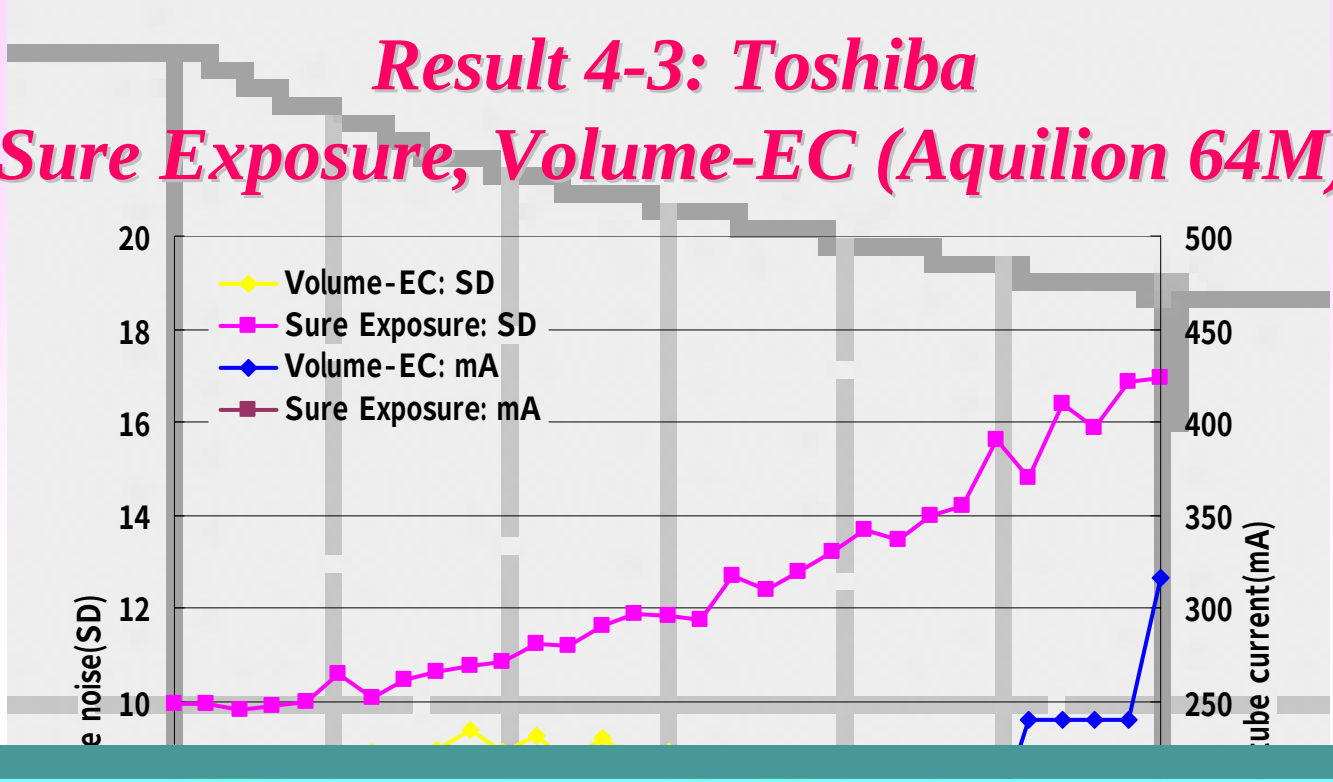

Figure 26 shows the patient shape characteristics obtained when the variable-XY phantom was scanned in the IN direction.

For Sure Exposure, the ROI-SD increased significantly as the vertical-to-horizontal ratio became larger.

For Volume-EC, the ROI-SD showed an almost constant value of 8.4 regardless of the vertical-to-horizontal ratio.

Result 4-4: Toshiba Sure Exposure, Volume-EC (Aquilion 64M)

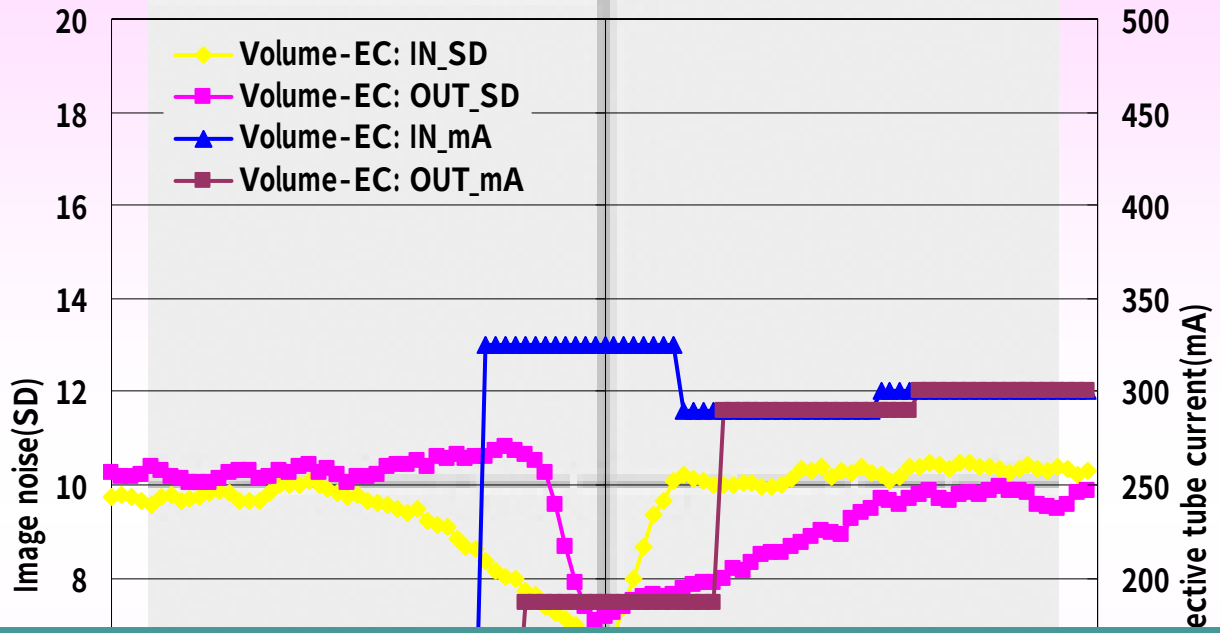

Figure 27 shows the response characteristics of Volume-EC when the stepped phantom was scanned.

In both IN and OUT scanning, the ROI-SD changed significantly at the origin point where the phantom diameter changed, but showed a value approximately equal to or less than the set SD value of 10.0.

Discussion 1-1: GE

Auto mA, 3D mA (LightSpeed VCT)

As in the case for Sure Exposure and Volume-EC, with ideal operation of Auto (2D) mA, the preset SD can be obtained for the patient size and changes in shape. Although in 2D mA modulation is performed only in the Z-axis direction, the results obtained were equivalent to those for 3D mA.

This indicates that in 2D mA correction of the ellipse was performed appropriately by tube current modulation.

In 3D mA, the same ROI-SD could be obtained at an exposure dose approximately 15% lower when the phantoms with elliptical cross sections were scanned.

This demonstrates that 3D modulation contributes to exposure dose reduction.

Discussion 1-2: GE

Auto mA, 3D mA (LightSpeed VCT)

With regard to the patient thickness characteristics of the cone and elliptical cone phantoms, the ROI-SD was maintained at an almost constant level for the NI. However, it tended to be substantially lower than the NI, particularly at a larger BW.

The reason for this is considered to be a large rate of change in patient size, because the selected pitch factor is as high as 1.375 and the tube current is controlled taking into consideration patient information obtained in the range of approximately one or two gantry rotations before and after the target position.

From the above, when Auto mA (2D) and 3D mA are used in clinical practice, it is important to select an appropriate preset NI. In particular, the actual image noise tends to be superior to the NI. It is therefore necessary to pay close attention to the results of comparison.

Discussion 2-1: Phillips

Dose Right (Brilliance 16P)

In ACS, the positioning image is used to determine the maximum tube current based on the data for the standard body size converted to a comparable water-equivalent material and the obtained maximum tube current is then applied to D-DOM and Z-DOM.

In the present field tests, we selected the scan conditions under which the maximum tube current was set for the plane of the maximum phantom diameter in the scan range or a tube current providing an appropriate ROI-SD range was set for the plane of the lowest X-ray transmission rate in order to avoid any influence of ACS operation on the assessment of D-DOM and Z-DOM operation.

D-DOM is an AEC function that is very similar to Siemens's CARE Dose (not CARE Dose 4D) and is designed so that image noise is reduced to a level comparable to that of images with AEC Off regardless of the phantom size and shape.

Discussion 2-2: Phillips

Dose Right (Brilliance 16P)

The tube current at this time is at least lower than that with AEC Off, providing a lower exposure dose while maintaining a level of image quality comparable to that of images with AEC Off.

On the other hand, the test results for the cone, elliptical cone, and variable-XY phantoms showed that Z-DOM recognizes the patient size in terms of area (same as for Sure Exposure), resulting in the same tube current value for the same planar area. Therefore, image noise in the plane varies depending on the patient shape, but it is obvious from the results for the elliptical cone phantom that this can be improved by using the Adaptive Filter in combination.

From the above findings, when Dose Right is used in clinical practice, it is important to select the standard image for ACS in order to ensure high image quality at a low exposure dose. However, D-DOM and Z-DOM have both advantages and disadvantages, and the provision of a 3D AEC function is therefore eagerly awaited.

Discussion 3-1: Siemens

Care Dose 4D (Sensation 64)

In CARE Dose 4D, the Ref. mAs entered by the user is used to determine the degree of modulation in the Z direction based on the patient information from the positioning image (Topogram) and the degree of modulation in the rotation-angle direction (XY plane) from the opposed-beam data during scanning.

The slope of the ROI-SD for CARE Dose 4D was constant with changes in patient size but was obviously milder than that with AEC Off.

This is considered to reflect a design concept in which the exposure dose should be effectively reduced without a significant deterioration in image quality so as to maintain image quality comparable to that with AEC Off.

Discussion 3-2: Siemens

Care Dose 4D (Sensation 64)

In comparisons between the cone phantom and the elliptical cone phantom, the ROI-SD for the elliptical cone phantom showed lower values.

For the variable-XY phantom, when the vertical-to-horizontal ratio increased, the ROI-SD with AEC Off was increased slightly, while the ROI-SD for CARE Dose 4D was reduced.

The reason for this is that the Sensation 64 automatically applies an adaptive filter as the vertical-to-horizontal ratio increases.

It is therefore considered that for CARE Dose 4D this filter processing and tube current modulation were superimposed.

From the above, when CARE Dose 4D is used in clinical practice, it is important to select an appropriate Reference mAs as well as to consider the contribution of the image noise variation range due to modulation intensity factors in clinical images.

Discussion 4-1: Toshiba

Sure Exposure, Volume-EC (Aquilion 64M)

With ideal operation of both Sure Exposure and Volume-EC, the preset SD can be obtained for the patient size and changes in shape. In Volume-EC,an SD value almost equal to the preset value could be obtained regardless of the phantom type. In Sure Exposure, however, the ROI-SD tended to increase to a value higher than the preset SD when the vertical-to-horizontal ratio was large.

The reason is that in Sure Exposure the tube current is modulated for every rotation by approximation to a circle at each slice position, while in Volume-EC the tube current is modulated according to the rotation angle by approximation to an ellipse at each slice position.

Moreover, Sure Exposure makes it possible to improve image quality at the lung apex and in the pelvis by using the RASP processing function (a type of adaptive processing function) in combination.

Discussion 4-2: Toshiba

Sure Exposure, Volume-EC (Aquilion 64M)

The test results for the stepped phantom showed that in Volume-EC modulation is performed beforehand based on the positioning image at a slice position where the patient size changes significantly.

This means that image quality is given priority in the case of a significant change in size such as at the lung apex or in regions near the diaphragm.

From the above, when Sure Exposure and Volume-EC are used in clinical practice, it is important to select an appropriate preset SD in order to ensure high image quality at a low exposure dose.

Conclusion

In order to establish a method for evaluating CT-AEC performance, our research group has conducted initial tests using special phantoms.

Our experimental results have demonstrated that the CT-AEC systems employed by the manufacturers provide a means to reproducibly control image quality, and the potential to optimize patient dose.

However, the performance characteristics that have been clarified in this study were found to differ markedly.

In order to ensure that these systems are employed properly in clinical practice, namely, to minimize the exposure dose while maintaining image quality, it is important to have a clear understanding of the features and to select the appropriate parameters.

It is obvious that the operation of these systems is far from fully automatic.